Validation and tuning of prognostic convection inside 3MT

Doina Banciu, National Meterological Administration - Romania
Stay Report: Prague, 20 August- 29 September 2007

Supervisor: Radmila Brozkova

1. Introduction

An important work was previously done at CHMI for the validation of 3MT part of ALARO-0, leading to a “relative” stable code of the prognostic convection and to a basic set-up for ALARO0 including 3MT part.

The existence of a reference version ALARO-0 without 3MT (so called “LSTRAPRO”, operational at CHMI, from January 2007) and of the diagnostic and verification tools have already allowed the identification of some problems related to 3MT:

- A strong water phase convective condensation at higher levels
- A strong negative value correction for liquid water, indicated an inconsistency between the transport and condensation terms

The further validation and tuning of the prognostic convection carried out in August-September 2008 was a teamwork effort involving Radmila Brozkova and Jean-Francois Geleyn and co-operation with Luc Gerard.

2. Further validation and tuning

The existence of DDH tools (adapted by Tomislav Kovacik for the ALARO frame) and the existence of the “LSTRAPRO” reference version of ALARO-0 played a crucial role during the validation and preliminary tuning work.

2.1 Discretization of the convective condensation and transport fluxes:

For the analysis the budgets of temperature, water phases and wind have been computed over a domain with significant convection activity (domain A from the figure1), for a day with strong convective activity, 21st of June 2006. The comparison between 3MT experiments and experiments where the diagnostic cloud profile characteristics were injected in the prognostic updraft and downdraft proved the existence of problems inside the convective condensation and transport computations.

Indeed after the modification of the discretization inside the condensation computation to be fully compatible with that of updraft transport one (upstream implicit) and the inversion of sense of the downdraft transport computation (see Annex 1), the syndrome of negative liquid water correction disappeared and a better temperature and humidity equilibrium was achieved for medium troposphere (figures 2 and 3). One can notice the enhanced level of the convective activity, not unexpected by passing from diagnostic to prognostic convection.

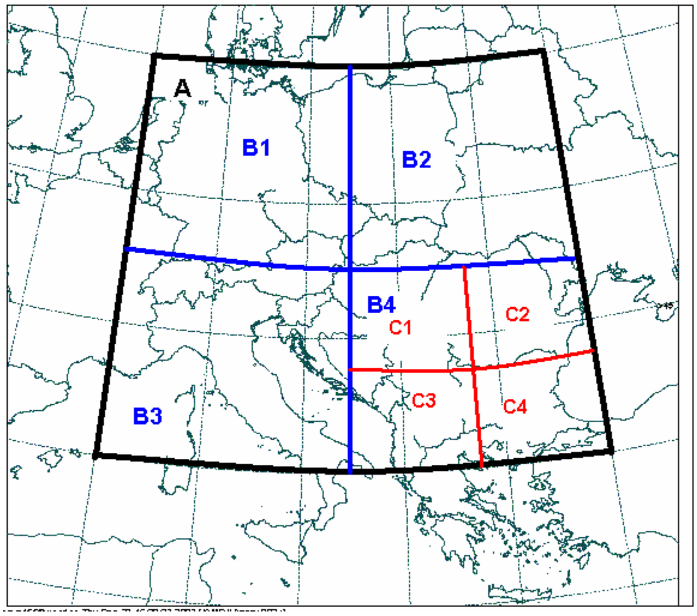

Fig.1: Different domains for the DDH computation

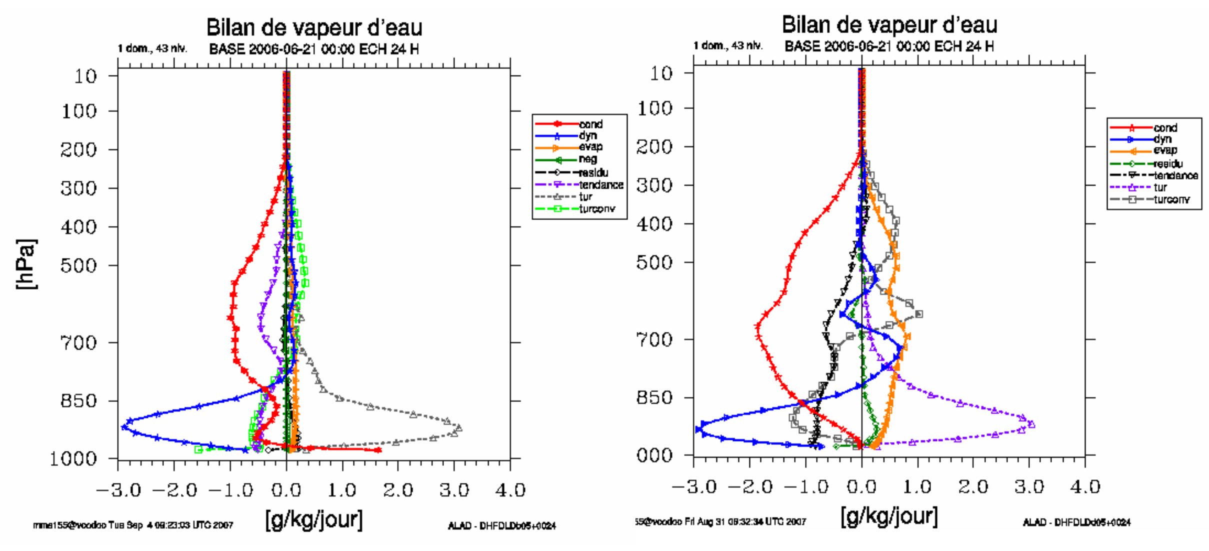

Fig.2: Water vapour budget: ALARO-0 without 3MT (left: red-condensation , green-convective transport, violet-tendency) and with 3MT (right: red-condensation flux, grey-convective transport flux, black-tendency) 21.06.2006, 00+ 24h

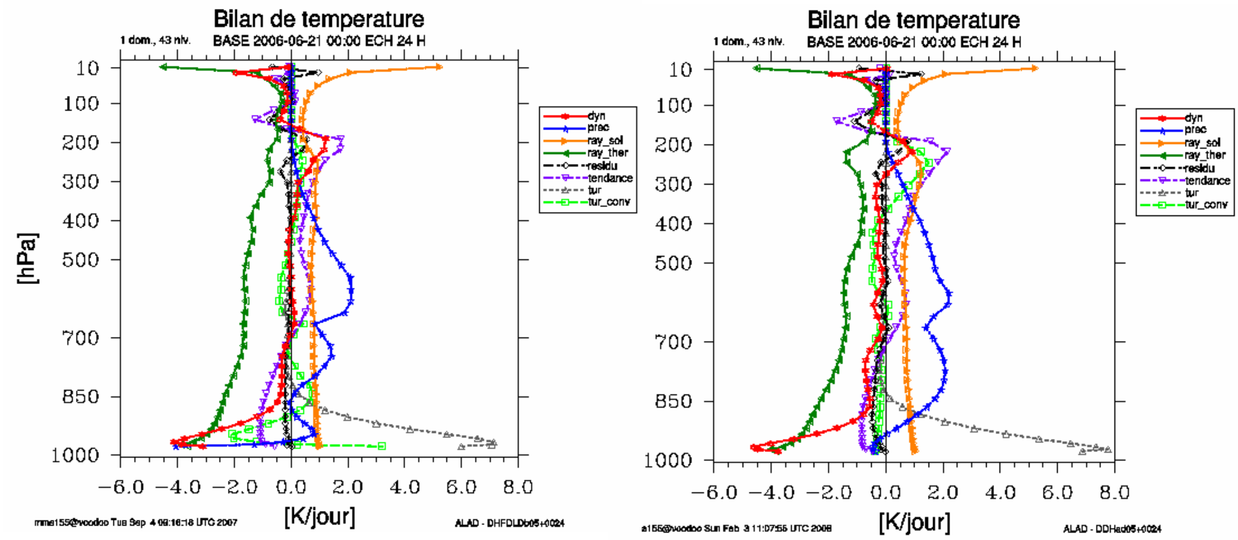

Fig.3 Temperature budget: ALARO-0 for 21.06.2006, 00+ 24h, without 3MT (left) and with 3MT (right): violet-tendency, light green-convective transport, dark green-thermal radiation

2.2 Tuning of the free parameters after the dicretization change

After the above mentioned corrections there were still some deficiencies: too much moist static energy in the upper atmosphere and too dry low levels (see figures 2 and 3), supposed to be reduced trough the tuning of the free parameters.

A tuning of the parameters was carried out in order to improve the budgets structure, by using again DDH tools. An important difference of the sensitivity of diagnostic and prognostic convection on the entrainment parameters was revealed. The different impact (bigger for prognostic convention; for temperature mainly in the medium troposphere and for humidity in the lower troposphere) of the same variation of the entrainment rate (TENTR and TENTRX) can be seen on the figures 4 and 5. It is worth to mention that the “ensemble” entrainment parameter, GCVNU, was set to 1e-05 (in respect with 2.5e-05, actual setting).

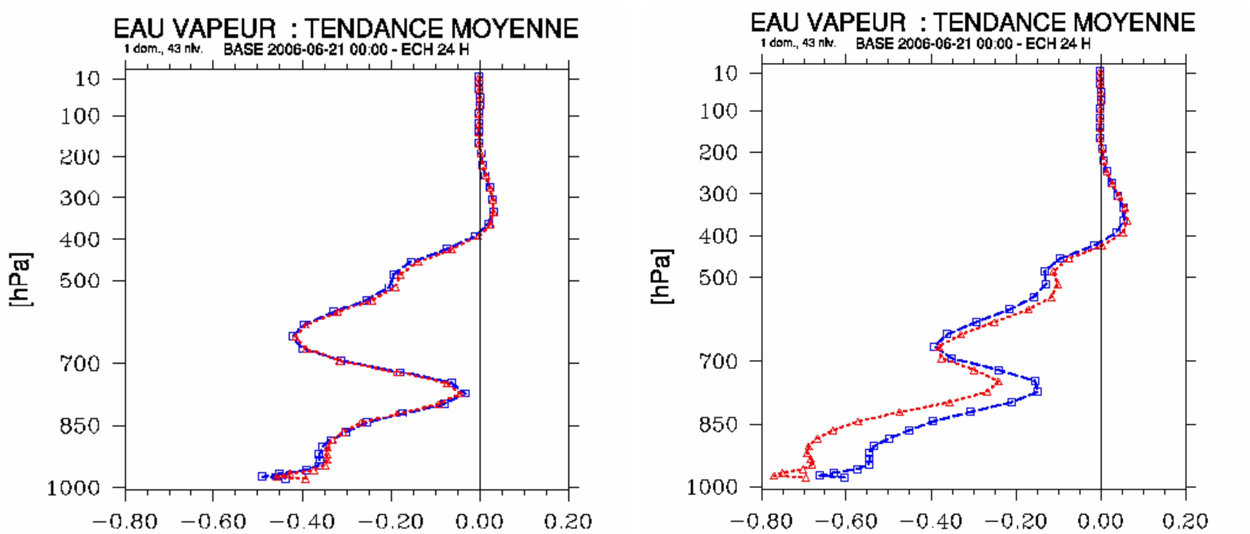

Fig.4: Water vapour tendency for two entrainment rates for 21.062006, 00+24 h: ALARO without 3MT part (left) and with 3MT (right); GCVNU=1.e-05, red - TENTR=2.5e-06, TENTRX=8.e-05 (actual setting), blue - TENTR=5e-06, TENTRX=16e-05,

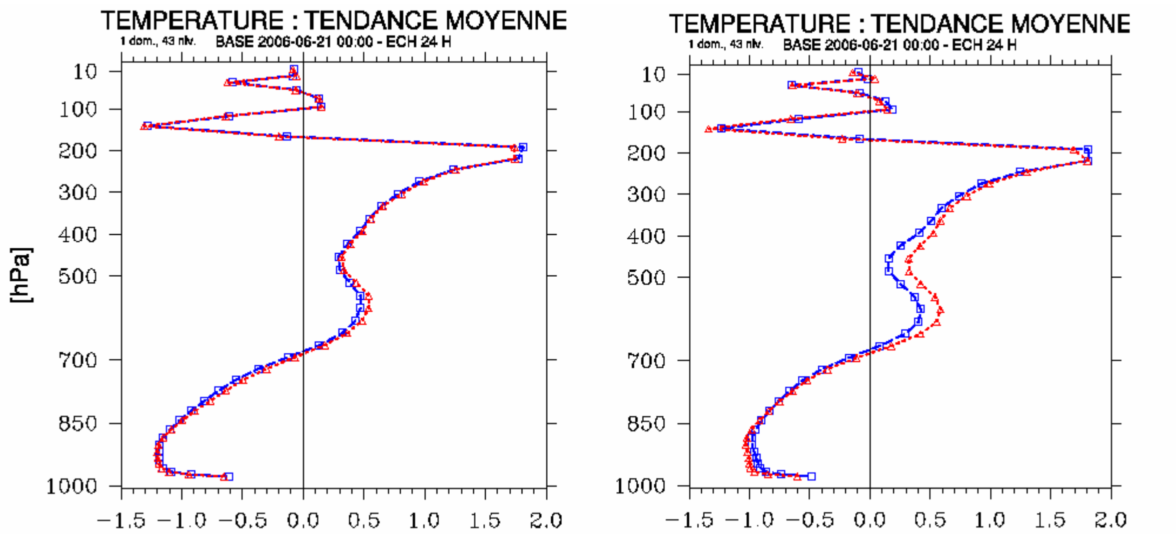

Fig.5: Temperature tendency for two entrainment rates for 21.062006, 00+24 h: ALARO without 3MT part (left) and with 3MT (right), red TENTR=2.5e-06,TENTRX=8.e-05 (reference), blue- TENTR=5e-06,TENTRX=16e-05

As well a preliminary tuning of the auto conversion rates (RAUTERFR, RAUTERFS) was done. On the other hand low sensitivity of prognostic convection on varying other parameters like friction parameter (TUDFR) prognostic updraft velocity was found.

2.3 The net condensation rate within the prognostic updraft ascent

During the tuning process other small bugs were corrected but the were still deficiencies, especially in the 500-700 hPa layer. By injection only of the diagnostic mass flux in the prognostic updraft routine and comparisons with the "LSTRAPO" results, it appeared that a problem remained in the computation of the updraft profile.

A special attention was given to the computation of the net condensation rate within the updraft ascent. In the original formulation the mixing with the environmental air was taking into account only for the water vapour and not for temperature. The modifications carried out were based on the idea of Jean-Marcel Piriou developed in his PhD thesis ("Representation de la convection dans les modeles globaux et regionaux: concepts, equations, etudes de cas") by considering primarily the adjustment to a saturated state (versus mixing processes). Practically this involved the computation of the mixing of the saturated values of water vapour and temperature before the convective ascent and the update of these values before calling of the prognostic updraft routine (as for the other thermodynamical variables). The update of the saturated variables was done as well before the microphysics and prognostic downdraft computations, where the same function for the partition between ice and liquid water as in convective drafts computations was used. Further, the convergence of the Newton algorithm of the saturated adiabat computation was improved by a consistent us of the temperature dependency inside the thermodynamic functions.

The impact of the modifications was checked with the help of DDH and again a tuning was performed for the parameters related to the entrainment: minimum and maximum entrainment rates (TENTR, TENTRX), the coefficient for entrainment rate computation from cloud buoyancy GCVALFA) and the "ensemble" entrainment. These lead to the diminution of one of the important deficiencies: too high temperature around 250-hPa level.

With the preliminary tuning and all correction included a parallel suite LSTRAPO/3MT (including surface data assimilation) for the period 21-31.06.2006 was carried out by Radmila. The activation of the prognostic was encouraging: the precipitation field for 21.06.2008 is better structured in the case of prognostic convection (fig.6). As well the RMSE score (computed against observation) are neutral or better, except for relative humidity in the 500-250 hPa layer (figure 7).

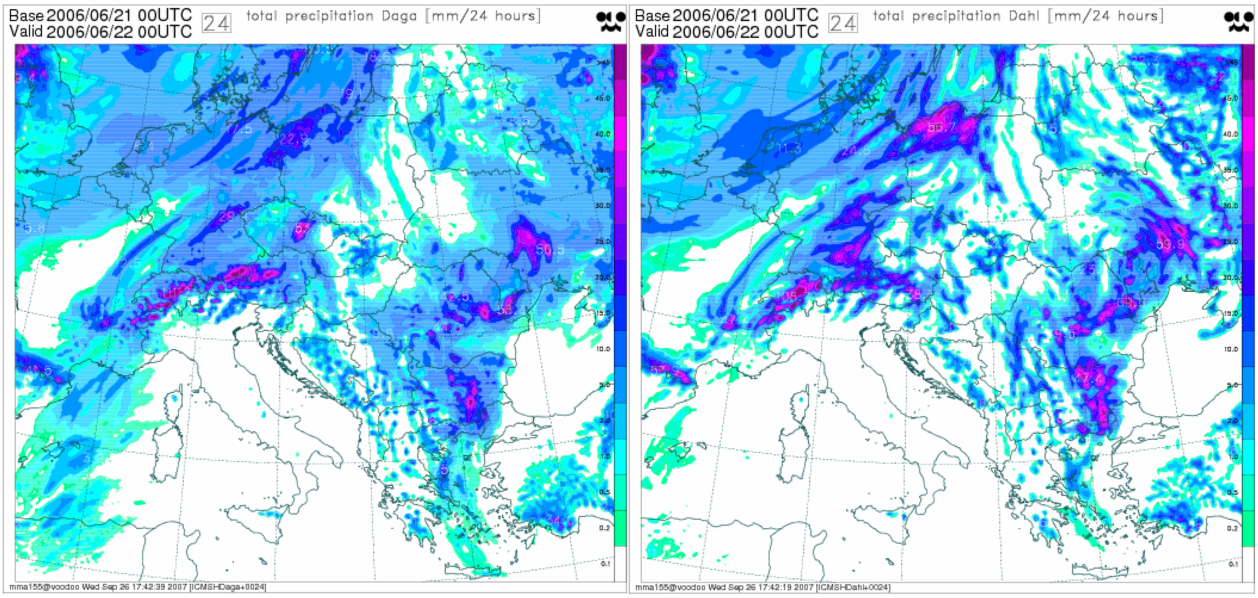

Fig.6: Cumulated precipitation: LSTRPRO-left, 3MT-right, 21.062006, 00 UTC + 24h

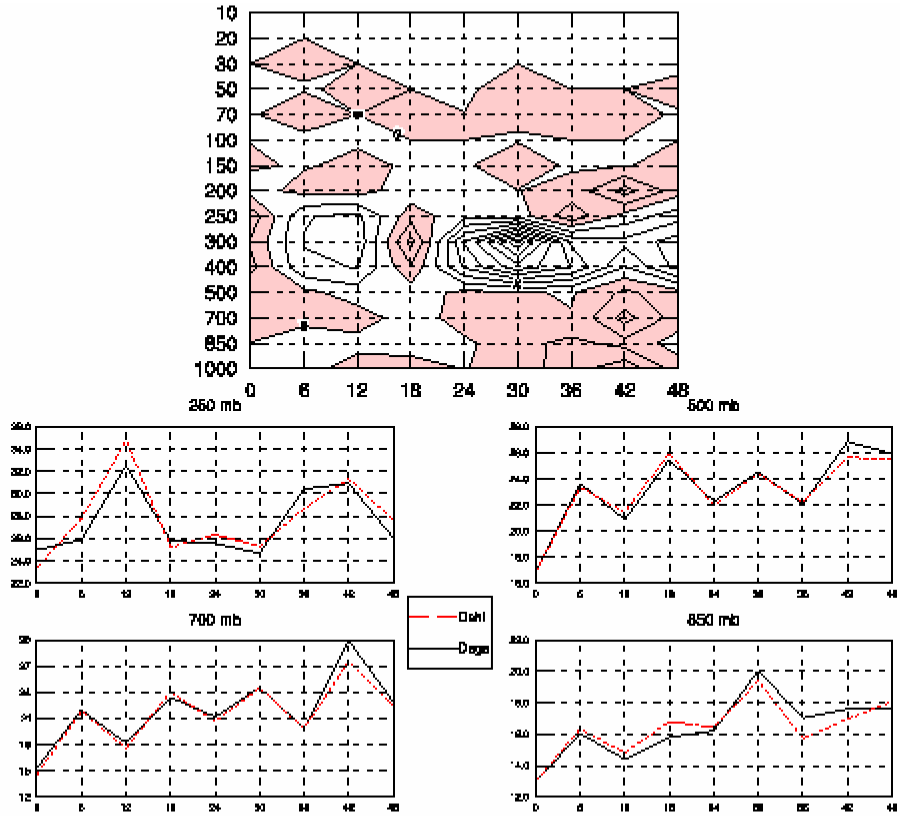

Fig.7: Evolution of the relative humidity RMSE with the forecast range (bottom; black-LSTRAPO, red-3MT), RMSE differences 3MT-LSTRAPO (center: red-score improvement), 21-30.062006

In the BIAS scores (shown in figures 8-9), the defficiences of the relative humidity and temperature are more pregnant.

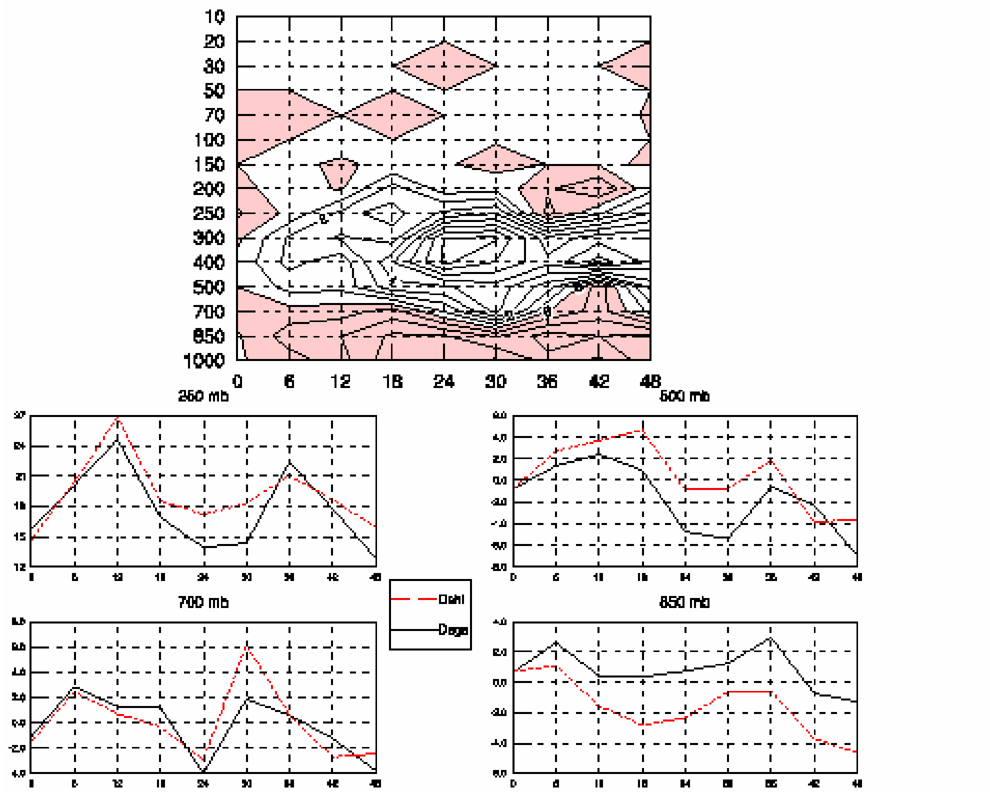

Fig.8: Evolution of the relative humidity BIAS with the forecast range (bottom; black-LSTRAPO, red-3MT), BIAS differences 3MT-LSTRAPO (center: red-score improvement), 21-30.062006

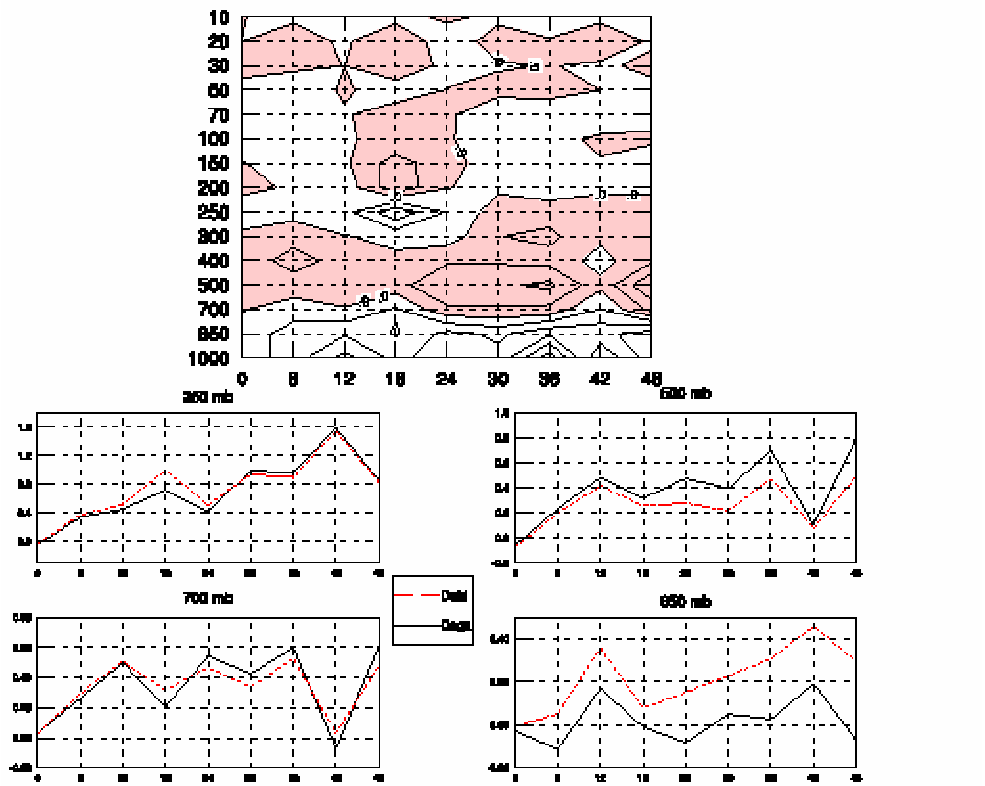

Fig.9: Evolution of the temperature BIAS with the forecast range (bottom; black-LSTRAPO, red-3MT), BIAS differences 3MT-LSTRAPO (center: red-score improvement), 21-30.062006

2.4 The specific problem of the 500-700 hPa layer

The main remained deficiencies concerned the 500-700 hPa layer. DDH showed that at least part of these deficiencies were linked to a sudden convergence of the convective momentum flux in the zone of mixed water phases (see fig. 10 and 11).

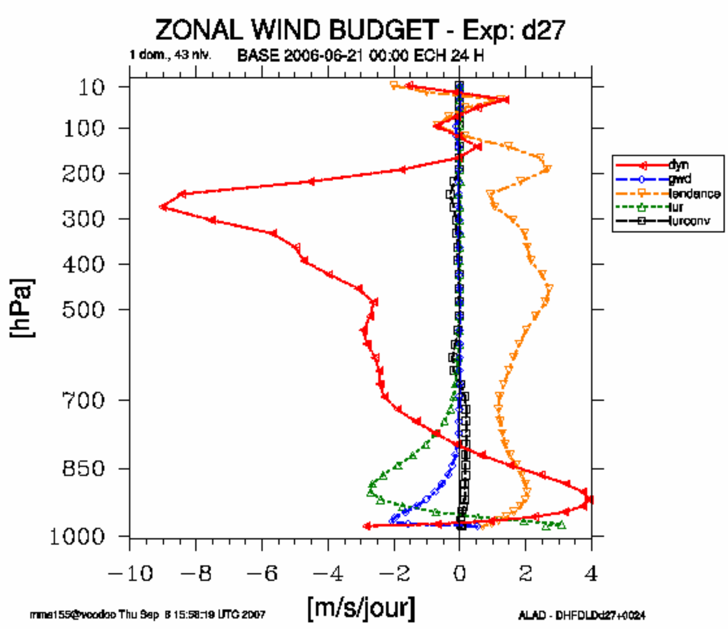

Fig.10: Momentum budget (u component) with prognostic convection (3MT), 21.06.2006, 24h integration

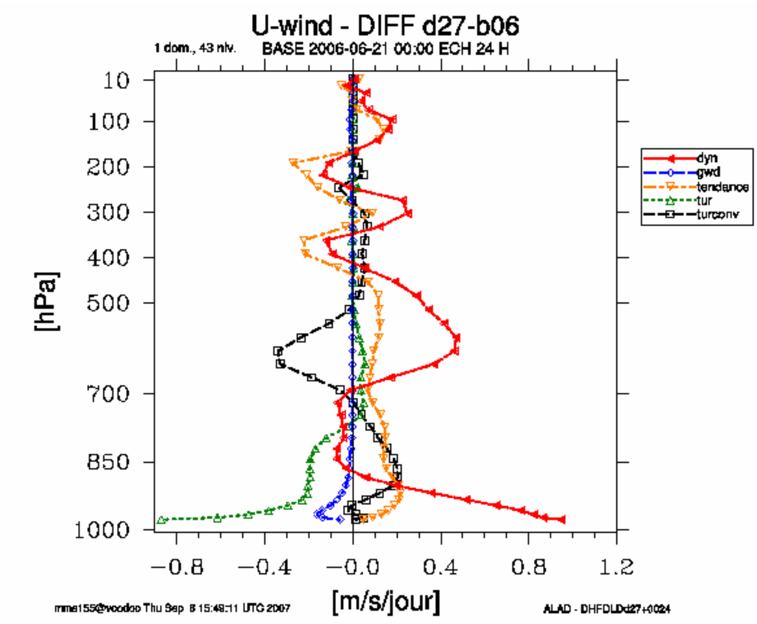

Fig.11: Momentum budget (u component) difference: 3MT- LSTRAPRO, 21.062006, 24h integration

The momentum flux behaviour was supposed to be linked to a mass flux problem. Therefore specific diagnostics on mass flux, again with the help of DDH tool: the updraft and downdraft mass fluxes were stored in the convective momentum flux variables, for what the budgets were computed. During the tests an error was found in the discretization of the auto-advection term in the vertical velocity equation of the prognostic updraft (see Annex 2) and similar for the downdraft. The impact of this modification on the updraft mass flux, especially in the critical zones (around 250 hPa and 700 hPa) can be seen on figure 12.

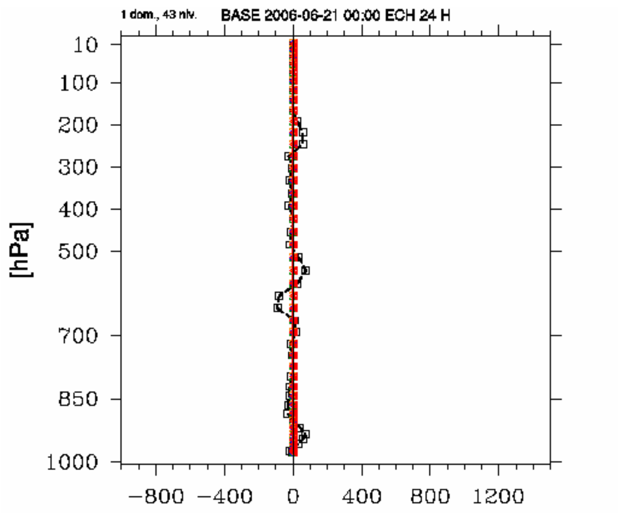

Fig.11: Mass flux gradient difference between 3MT after and before correction of the omega equation, 21.062006, 24h integration

For a deeper study of the momentum flux the basic domain for the DDH (labelled A in fig. 1) was successively divided in smaller parts (labelled B and C) in order to find an area where the syndrome was more pregnant. The chosen domains were C3 on what the updraft mass fluxes with and without prognostic convection were compared (fig.12) only for 12-hour integration (found to be enough for the manifestation of the syndrome).

Other diagnostic have been done as well on the same domain: the distribution of the total and convective precipitation, thermal radiation at atmosphere, temperature and wind at different levels (for instance fig.13) in order to isolate the points with the main contribution in the budget behaviour. For a better determination of the problem a test without mass flux advection was carried out: in the precipitation field the (fig.14), the "storm point" is more obvious. For few selected points, the parameters controlling the updraft stopping on the vertical where checked, by direct print of the values at certain moments (thanks to code modifications made by Radmila to allow it).

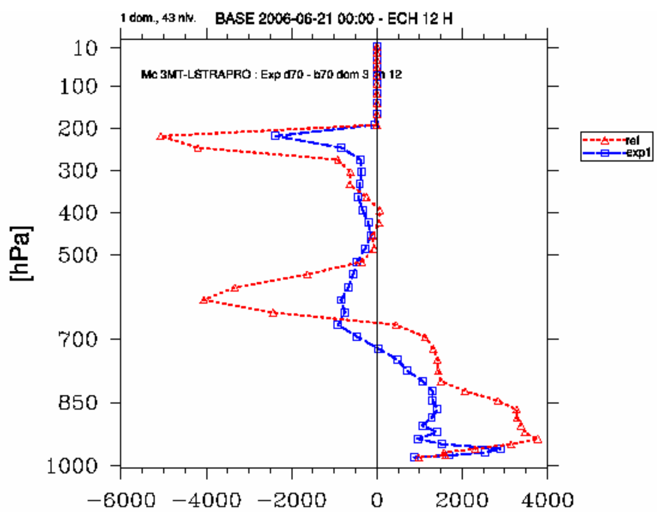

Fig.12: Mass flux gradient for the domain C3: red-3MT, blue-LSTRAPRO, 21.062006, 12h integration

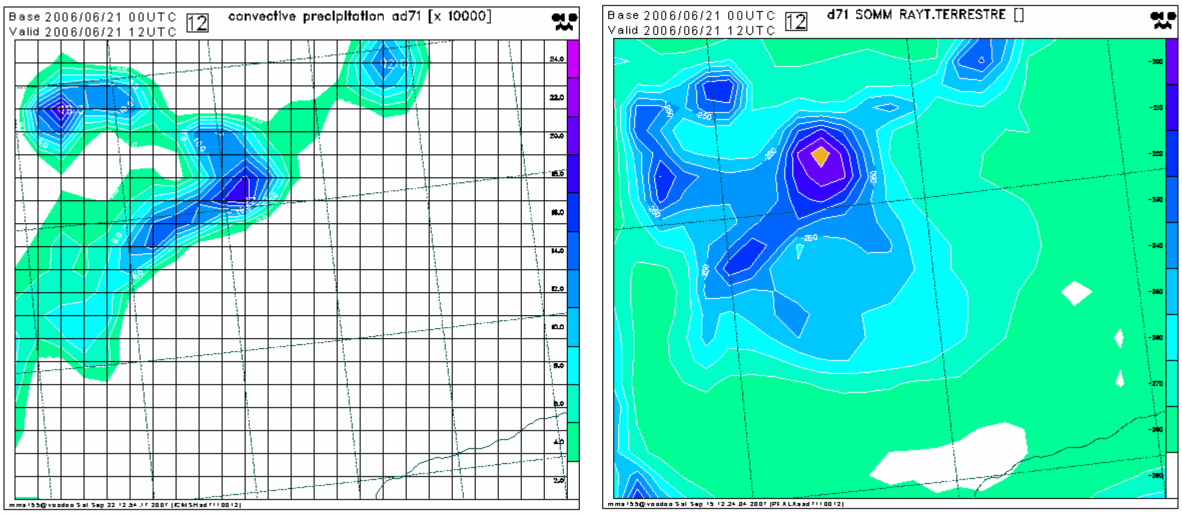

Fig. 13. Instantaneous convective precipitation (left) and thermal radiation at atmosphere top (right) zoom on the C3 domain, 21.06.2006, 12 h

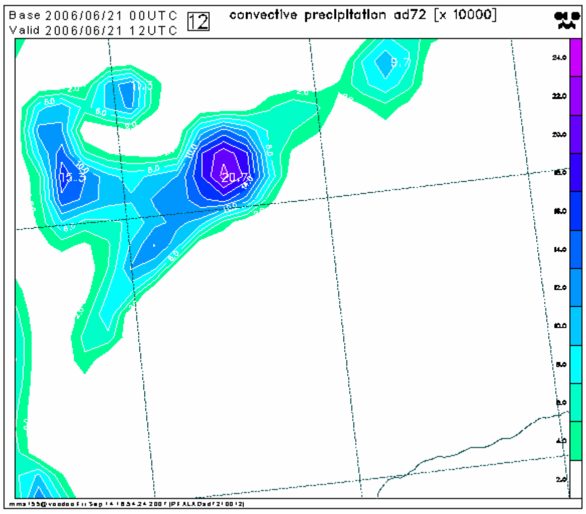

Fig. 14. Instantaneous convective precipitation for an experiment with no advection of the mass flux, zoom on the C3 domain, 21.06.2006, 12 h

Another direction for a possible explication of mass flux syndrome was the link with microphysics. The diagnostics made by Luc Gerard on the same case showed:

- a cold peak below the triple point generated by the precipitation melting, with a big effect on the updraft velocity through the enhanced buoyancy. of the updraft;
- a negative peak for the convective dry static and moisture transport fluxes inducing a reduction of the buoyancy at the bottom of the mixed layer, through warming and moistening effect;

Several tests were done by modifying the melting-freezing degree around the triple point via a parameter (ZGELM) varying from 0 to 1000. The mass flux budgets computed after 24-hour integration, over the entire DDH domain proved the bigger impact on the level of interest (figure 15).

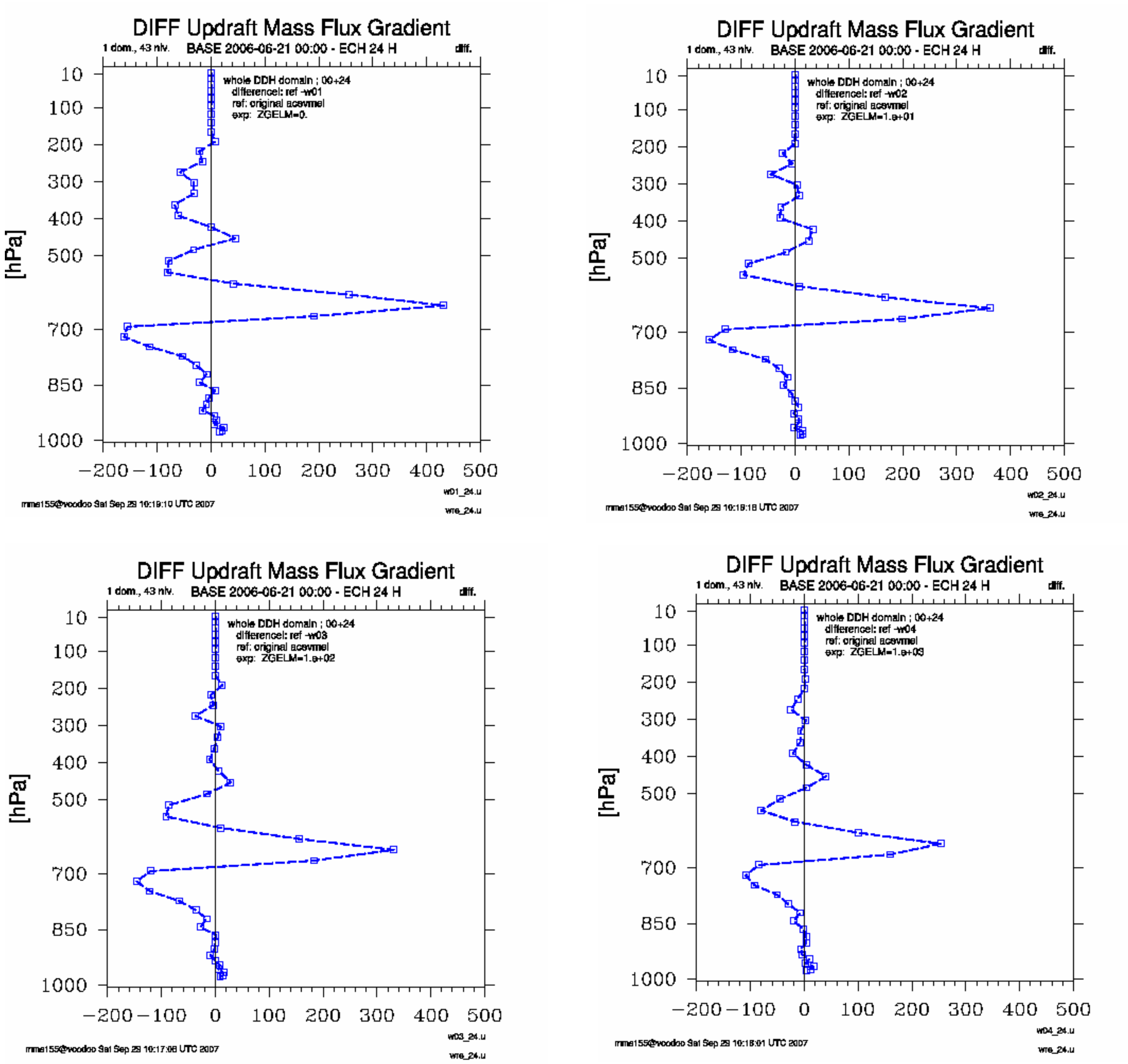

Fig.15 Mass flux gradient differences between the melting/freezing experiments and the reference formulation: top left - ZGELM=0 (no re-freezing) , top-right - ZGELM=10, bottom right - ZGELM=100, bottom right - ZGELM=1000

3. Summary

The work carried out during August-September 2007, tried to solve the problems found previously in the formulation of prognostic convection by approaching the discretization of condensation fluxes, computation of brute condensation rate and link with microphysics. The problem of the cloud top penetration remained under the investigation, the actual solution not being very physical.

Even if the problems were not entirely solved, a further step in the validation and tuning of ALARO-0 including3MT part was done.

Final set-up of the free parameters at the end of September 2007

After all modifications described above a new tuning was search. Several other free parameters were touched during the tuning process, some of them having a small impact, as the value of the minimum advected updraft velocity for the consideration of the convective activity independent on the buoyancy (GCVACHI). The best results were found for the following combination:

GDDEVF=0.25
GCVALFA=3.e-05
TENTR=5.e-06
TENTRX=16e-05
GCVNU=1.e-05
RAUTERFR=2.e-03
RAUTERFS=2.e-03

Acknowledgements

I am grateful to Radmila Brozkova and Jean-Francois Geleyn for the very fruitful discussions, for proposing new ideas/solutions and constant support of my work. As well, many thanks to the members of Czech Aladin team for their help in using the available tools and their effort to make comfortable my stay at CHMI.

References

Gerard, L., 2007: An integrated package for subgrid convection, clouds and precipitation compatible with the meso-gamma scales, *accepted in Q.J.R.Meteorol.Soc*

Gerard, L.; Geleyn, J.F., 2005: Evolution of a subgrid deep convection parametrization in a limited-area model with increasing resolution -Source: *Quarterly Journal of the Royal Meteorological Society, Number 610, July 2005 Part B, pp. 2293-2312(20)*

Gerard, L., 2001: Physical Parameterisations for a high resolution operational Numerical Prediction Model, *PhD Thesis, Université libre de Bruxelles*

Gerard, L., 2007: personal documentation on updraught, *www.rclace.eu*

Gerard, L., 2007: personal documentation on downdraught, *www.rclace.eu*

Piriou, J-M., 2006, Représentation de la convection dans les modèles globaux et régionaux: concepts, équations, études de cas, Ph.D thèse, Université Paul Sabatier, Toulouse, France

ANNEX 1

TURBULENT TRANSPORT AND CON DENSATION / EVAPOATATION OF CONVECTIVE UPRDAFT AND MOIST DOWNDRAFT IN THE 3MT FRAME

1. Convective updraft

1.1. Convective transport fluxes

$$\frac{\partial \psi}{\partial t} = -\frac{\partial}{\partial p}\sigma_u \omega_u (\psi_u - \psi) = -\frac{\partial}{\partial p} M_u (\psi - \psi_u) = -g\frac{\partial J_\psi^{conv}}{\partial p} \qquad (1)$$

with $M_u = -\sigma_u \omega_u$

- ***Implicit computation; downward*** *(as implemented in ACCUVD)*

The discretized form of the equation 1 is:

$$\left(1 + \frac{c_{\bar{l}}}{\Delta p_l}\right)\psi_*^l - \frac{c_{\bar{l}-1}}{\Delta p_l}\psi_*^{l-1} = \psi^l + \frac{c_{\bar{l}-1}}{\Delta p_l}\left(\frac{\psi^l - \psi^{l-1}}{2} - \frac{\psi_u^l + \psi_u^{l-1}}{2}\right) - \frac{c_{\bar{l}}}{\Delta p_l}\left(\frac{\psi^{l+1} - \psi^l}{2} - \frac{\psi_u^{l+1} + \psi_u^l}{2}\right) \qquad (2)$$

where $c = M_{u.} \Delta t$,

or in an equivalent form:

$$\psi_l^* = \frac{\Delta p_l}{\Delta p_l + c_{\bar{l}}}\left[\psi^l + \frac{c_{\bar{l}-1}}{\Delta p_l}\left(\psi_{\bar{l}-1}^* + \frac{\psi^l - \psi^{l-1}}{2} - \frac{\psi_u^l + \psi_u^{l-1}}{2}\right) - \frac{c_{\bar{l}}}{\Delta p_l}\left(\frac{\psi^{l+1} - \psi^l}{2} - \frac{\psi_u^{l+1} + \psi_u^l}{2}\right)\right] \qquad \text{(2 bis)}$$

$$-g\Delta t\left(\Delta J_\psi^{conv}\right)_l = \Delta p_l \cdot \left(\psi_l^* - \psi_l\right) = \frac{\Delta p_l}{\Delta p_l + c_{\bar{l}}}\left(c_{\bar{l}-1} A_{\bar{l}-1} - c_{\bar{l}} B_{\bar{l}}\right)$$

$$A_{l-1} = \left(\psi^*_{\bar{l}-1} + \frac{\psi^l - \psi^{l-1}}{2} - \frac{\psi^l_u + \psi^{l-1}_u}{2} \right) \quad B_l = \left(\frac{\psi^{l+1} + \psi^l}{2} - \frac{\psi^{l+1}_u + \psi^l_u}{2} \right)$$

$$J^{\bar{l}}_{\psi} = \frac{c_{\bar{l}}}{\Delta p_l + c_{\bar{l}}} \left[J^{\bar{l}-1}_{\psi} + \frac{\Delta p_l}{g \cdot \Delta t} \left(\frac{\psi^{l+1} + \psi^l}{2} - \frac{\psi^{l+1}_u + \psi^l_u}{2} \right) \right] \tag{3}$$

1.2. Condensation fluxes

Within the 3MT approach the computation of the condensate rate should be fully compatible with the convective turbulent one. To derive the respective implicit algorithm we should identify inside the discretized form of the convective transport the term corresponding to condensation, $M_c \dfrac{\partial \psi_u}{\partial p}$.

$$\frac{\partial}{\partial p}\left[M_u(\psi_u - \psi)\right] = (\psi_u - \psi)\frac{\partial M_u}{\partial p} + M_u \frac{\partial \psi_u}{\partial p} - M_u \frac{\partial \psi}{\partial p}$$

For an easier identification of the terms, the equation 2 can be rewritten as:

$$\left(1 + \frac{c_{\bar{l}}}{\Delta p_l}\right)\left(\psi^l_* - \psi^l_u\right) - \frac{c_{\bar{l}-1}}{\Delta p_l}\left(\psi^{l-1}_* - \psi^{l-1}_u\right) = \psi^l - \psi^l_u + \frac{c_{\bar{l}-1}}{\Delta p_l}\left(\frac{\psi^l - \psi^{l-1}}{2} - \frac{\psi^l_u - \psi^{l-1}_u}{2} \right) - \frac{c_{\bar{l}}}{\Delta p_l}\left(\frac{\psi^{l+1} - \psi^l}{2} - \frac{\psi^{l+1}_u - \psi^l_u}{2} \right) \tag{4}$$

a) To eliminate the term $(\psi_u - \psi)\dfrac{\partial M_u}{\partial p}$ one has to replace $c_{\bar{l}}$ in the first term of the LHS of equation for by $c_{\bar{l}-1}$

$$\left(1 + \frac{c_{\bar{l}-1}}{\Delta p_l}\right)\psi^l_* - \frac{c_{\bar{l}-1}}{\Delta p_l}\psi^{l-1}_* = \psi^l + \frac{c_{\bar{l}-1}}{\Delta p_l}\left(\frac{\psi^l - \psi^{l-1}}{2} + \frac{\psi^l_u - \psi^{l-1}_u}{2} \right) + \frac{c_{\bar{l}}}{\Delta p_l}\left(\frac{\psi^{l+1} - \psi^l}{2} - \frac{\psi^{l+1}_u - \psi^l_u}{2} \right) \tag{5}$$

b) Further, by ignoring the ψ terms, the implicit formulation for the condensation term is obtained:

$$\left(1+\frac{c_{\bar{l}-1}}{\Delta p_l}\right)\psi_*^l - \frac{c_{\bar{l}-1}}{\Delta p_l}\psi_*^{l-1} = \frac{c_{\bar{l}-1}}{\Delta p_l}\left(\frac{\psi_u^l - \psi_u^{l-1}}{2}\right) + \frac{c_{\bar{l}}}{\Delta p_l}\left(\frac{\psi_u^{l+1} - \psi_u^l}{2}\right) \qquad (6)$$

The explicit formulation of the condensation rate can be written as:

$$CR_{expl}^l = \frac{1}{g\Delta t\Delta p_l}\left[c_{\bar{l}-1}\left(\frac{q_u^l - q_u^{l-1}}{2}\right) + c_{\bar{l}}\left(\frac{q_u^{l+1} - q_u^l}{2}\right)\right] \qquad (7)$$

Consequently, the implicit condensation rate is given by:

$$\left(1+\frac{c_{\bar{l}-1}}{\Delta p_l}\right)CR_*^l = \frac{c_{\bar{l}-1}}{\Delta p_l}\cdot CR_*^{l-1} + CR_{expl}^l \qquad (8)$$

and the condensation flux by:

$$F_{cond}^l = F_{cond}^{l-1} + \Delta p_l \cdot CR_*^l \qquad (9)$$

c) Alternatively if the ψ_u terms are ignored in the equation 5, the discretization of the sole $-M_c\frac{\partial\psi_u}{\partial p}$ is obtained, as is currently implemented in ACCVIMP.

$$\left(1+\frac{c_{\bar{l}-1}}{\Delta p_l}\right)\psi_*^l - \frac{c_{\bar{l}-1}}{\Delta p_l}\psi_*^{l-1} = \psi_l + \frac{c_{\bar{l}-1}}{\Delta p_l}\left(\frac{\psi^l - \psi^{l-1}}{2}\right) - \frac{c_{\bar{l}}}{\Delta p_l}\left(\frac{\psi^{l+1} - \psi^l}{2}\right) \qquad (10)$$

2. Moist downdraft

The same algorithm is to be applied to the moist downdraft turbulent transport and evaporation fluxes.
NB. To assure the stability of the algorithm the computation has to be done upward.

2.1. Turbulent transport

$$\frac{\partial\psi}{\partial t} = -\frac{\partial}{\partial p}\sigma_d\omega_d(\psi_d - \psi) = -\frac{\partial}{\partial p}M_d(\psi_d - \psi) = -g\frac{\partial J_\psi^{conv}}{\partial p} \qquad (1')$$

$$M_d = \sigma_d \omega_d$$

- ***upward computation –***

$$\left(1+\frac{c_{\bar{l}-1}}{\Delta p_l}\right)\psi_*^l - \frac{c_{\bar{l}}}{\Delta p_l}\psi_*^{l+1} = \psi^l - \frac{c_{\bar{l}-1}}{\Delta p_l}\left(\frac{\psi^{l-1}-\psi^l}{2} - \frac{\psi_d^{l-1}+\psi_d^l}{2}\right) + \frac{c_{\bar{l}}}{\Delta p_l}\left(\frac{\psi^l-\psi^{l+1}}{2} - \frac{\psi_d^l+\psi_d^{l+1}}{2}\right) \quad (2')$$

where: $c = M_d \Delta t$

$$\psi_*^l = \frac{\Delta p_l}{\Delta p_l + c_{\bar{l}-1}}\left[\psi^l - \frac{c_{\bar{l}-1}}{\Delta p_l}\left(\frac{\psi^{l-1}-\psi^l}{2} - \frac{\psi_u^{l-1}+\psi_u^l}{2}\right) + \frac{c_{\bar{l}}}{\Delta p_l}\left(\psi_*^{l+1} + \frac{\psi^l-\psi^{l+1}}{2} - \frac{\psi_u^l+\psi_u^{l+1}}{2}\right)\right] \quad (2' \text{ bis})$$

$$-g\Delta t\left(\Delta J_\psi^{conv}\right)_l = \Delta p_l \cdot \left(\psi_l^* - \psi_l\right) = \frac{\Delta p_l}{\Delta p_l + c_{\bar{l}-1}}\left(c_{\bar{l}} A_{\bar{l}} - c_{\bar{l}-1} B_{\bar{l}-1}\right)$$

$$A_l = \left(\psi_*^{l+1} + \frac{\psi^l-\psi^{l+1}}{2} - \frac{\psi_u^l+\psi_u^{l+1}}{2}\right) \quad B_{l-1} = \left(\frac{\psi^{l-1}-\psi^l}{2} - \frac{\psi_d^{l-1}+\psi_d^l}{2}\right)$$

$$J_\psi^{\bar{l}-1} = \frac{c_{\bar{l}-1}}{\Delta p_l + c_{\bar{l}-1}}\left[J_\psi^{\bar{l}} + \frac{\Delta p_l}{g\cdot\Delta t}\left(\frac{\psi_d^{l-1}+\psi_d^l}{2} - \frac{\psi^{l-1}+\psi^l}{2}\right)\right] \quad (3')$$

2.2 Evaporation fluxes

$$\frac{\partial}{\partial p}\left[M_d\left(\psi_d - \psi\right)\right] = \left(\psi_d - \psi\right)\frac{\partial M_d}{\partial p} + M_d\frac{\partial \psi_d}{\partial p} - M_d\frac{\partial \psi}{\partial p}$$

The equivalent form of equation 4 is:

$$\left(1+\frac{c_{\bar{l}-1}}{\Delta p_l}\right)\left(\psi_*^l - \psi_d^l\right) - \frac{c_{\bar{l}}}{\Delta p_l}\left(\psi_*^{l+1} - \psi_u^{l+1}\right) = \psi^l - \psi_d^l - \frac{c_{\bar{l}-1}}{\Delta p_l}\left(\frac{\psi^{l-1}-\psi^l}{2} - \frac{\psi_d^{l-1}-\psi_d^l}{2}\right) + \frac{c_{\bar{l}}}{\Delta p_l}\left(\frac{\psi^l-\psi^{l+1}}{2} - \frac{\psi_d^l-\psi_d^{l+1}}{2}\right) \quad (4')$$

a) The discretization of $M_d \dfrac{\partial \psi_d}{\partial p}$ and $\psi_d \dfrac{\partial \psi_d}{\partial p}$ terms:

$$\left(1+\frac{c_{\bar{l}}}{\Delta p_l}\right)\psi_*^l - \frac{c_{\bar{l}}}{\Delta p_l}\psi_*^{l+1} = \psi_l - \frac{c_{\bar{l}-1}}{\Delta p_l}\left(\frac{\psi^{l-1}-\psi^l}{2} - \frac{\psi_d^{l-1}-\psi_d^l}{2}\right) + \frac{c_{\bar{l}}}{\Delta p_l}\left(\frac{\psi^l-\psi^{l+1}}{2} + \frac{\psi_d^l-\psi_d^{l+1}}{2}\right) \tag{5'}$$

b) The discretization of $M_d \dfrac{\partial \psi_d}{\partial p}$ (evaporation)

$$\left(1+\frac{c_{\bar{l}}}{\Delta p_l}\right)\psi_*^l - \frac{c_{\bar{l}}}{\Delta p_l}\psi_*^{l+1} = \frac{c_{\bar{l}-1}}{\Delta p_l}\left(\frac{\psi_d^{l-1}-\psi_d^l}{2}\right) + \frac{c_{\bar{l}}}{\Delta p_l}\left(\frac{\psi_d^l-\psi_d^{l+1}}{2}\right) \tag{6'}$$

The explicit formulation of the evaporation rate can be written as:

$$ER_{expl}^l = -\frac{1}{g\Delta t\Delta p_l}\left[c_{\bar{l}-1}\left(\frac{q_d^{l-1}-q_d^l}{2}\right) + c_{\bar{l}}\left(\frac{q_d^l-q_d^{l+1}}{2}\right)\right] \tag{7'}$$

Consequently, the implicit evaporation rate is given by:

$$\left(1+\frac{c_{\bar{l}}}{\Delta p_l}\right)ER_*^l = \frac{c_{\bar{l}}}{\Delta p_l}ER_*^{l+1} + ER_{expl}^l \tag{8'}$$

and the evaporation flux by:

$$F_{evap}^{l-1} = F_{evap}^l + \Delta p_l \cdot ER_*^l \tag{9'}$$

c) Alternatively if the ψ_d terms are ignored in the equation 5’, the discretization of the sole $-M_d \dfrac{\partial \psi_d}{\partial p}$ is obtained, as is currently implemented in ACCVIMPD.

$$\left(1+\frac{c_{\bar{l}}}{\Delta p_l}\right)\psi_*^l-\frac{c_{\bar{l}}}{\Delta p_l}\psi_*^{l+1}=\psi_l-\frac{c_{\bar{l}-1}}{\Delta p_l}\left(\frac{\psi^{l-1}-\psi^l}{2}\right)+\frac{c_{\bar{l}}}{\Delta p_l}\left(\frac{\psi^l-\psi^{l+1}}{2}\right) \qquad (10')$$

ANNEX 2

The discretization of the prognostic vertical velocity equation

The basic omega equation of the prognostic updraft

$$\left.\frac{\partial\omega_u^*}{\partial t}\right|_{ph} + (1_u - \sigma_u)\omega_u^*\left(\frac{\partial\omega_u^*}{\partial p} - \frac{\omega_u^*}{\pi} + \omega_u^*\frac{\partial \ln\overline{T_v}}{\partial p}\right) = \underbrace{\frac{g^2}{1+\gamma'}\frac{p}{R_a}\frac{T_{vu}-\overline{T_v}}{\overline{T_v}T_{vu}}}_{\text{buoyancy}} + \underbrace{\frac{\omega_u^{*2}}{p}R_a T_{vu}\left(\lambda+\frac{K_{du}}{g}\right)}_{\text{dissipation}}$$

can be written, by neglecting the with $\ln T_v$ term and the departure from hydrostatic pressure as (equation 37 of Luc Gerard' documentation):

$$\left.\frac{\partial\omega_u^*}{\partial t}\right|_{ph} = \frac{\omega_u^{*2}}{p}\left\{(1_u - \sigma_u) + R_a T_{vu}\left(\lambda+\frac{K_{du}}{g}\right)\right\} + \frac{(1_u - \sigma_u)}{2}\frac{\partial\omega_u^{*2}}{\partial p} - \frac{g^2}{1+\gamma'}\frac{p}{R_a}\frac{T_{vu}-\overline{T_v}}{\overline{T_v}T_{vu}}$$

or in the following symbolic form

$$\frac{\partial\omega_u^*}{\partial t} = A\omega_u^{*2} - \sigma_e\omega_u^*\frac{\partial\omega_u^*}{\partial p}$$

The problem is the discretization of the $\sigma_e\omega_u^*\frac{\partial\omega_u^*}{\partial p}$ term. This can be seen either as an advection term either as kinetic energy one. In the original formulation it was considered as an advection term the advection form (auto advection) supposed to be discretized similar to Geleyn-Girard-Louis (1982).

The term $\sigma_e\omega_u^*\frac{\partial\omega_u^*}{\partial p}$ is equivalent to $-M_c\frac{\partial\psi_u}{\partial p}$ from the Annex 1. The discretization should follow the equation 10 from the same Annex. However, there is a difference in the sense of the vertical loop, such as the discretization form is rather similar to those for downdraft, equation 10'. In respect with the diagnostic convective updraft (ACCVIMP routine) the vertical loop in ACCVUD has an opposite sense (upward). Therefore the discretization form is similar to those of downdraft (equation 10' from tce.doc) where the sign of c_l terms is to be changed. So, the equation 38 from the prognostic updraft documentation of Luc Gerard,

$$f_{n+1}^l - f_n^l = A^l\left(f_{n+1}^l\right)^2 - \frac{1}{\Delta p^l}\left\langle c_n^{\bar{l}}\left(f_{n+1}^{l+1} - \frac{f_n^{l+1} - f_n^l}{2}\right) - c_n^{\bar{l}-1}\left(f_{n+1}^l - \frac{f_n^l - f_n^{l-1}}{2}\right)\right\rangle$$

becomes,

$$f_{n+1}^l - f_n^l = A^l\left(f_{n+1}^l\right)^2 - \frac{1}{\Delta p^l}\left\langle c_n^{\bar{l}}\left(f_{n+1}^{l+1} - f_{n+1}^l - \frac{f_n^{l+1} - f_n^l}{2}\right) - c_n^{\bar{l}-1}\left(-\frac{f_n^l - f_n^{l-1}}{2}\right)\right\rangle$$

where the coefficient of the f_{n+1}^{l} term was changed from $c_n^{\bar{l}-1}$ in $c_n^{\bar{l}}$. Accordingly, the ZB equation is written as: $ZB \equiv B^{l+1} = 1 - \frac{c_n^{\bar{l}+1}}{\Delta p^l}$.